Soliton dynamics in photonic-crystal fibers with frequency-dependent Kerr nonlinearity

F. R. Arteaga-Sierra, A. Antikainen, and Govind P. Agrawal

Phys. Rev. A **98**, 013830 — Published 18 July 2018

DOI: 10.1103/PhysRevA.98.013830

Soliton dynamics in photonic crystal fibers with frequency-dependent Kerr nonlinearity

F. R. Arteaga-Sierra[1,*], A. Antikainen[1], and Govind P. Agrawal[1,2]
[1] *The Institute of Optics, University of Rochester, Rochester, New York 14627*
[2] *Laboratory for Laser Energetics, 250 East River Rd, Rochester, NY 14623*

We study numerically the evolution of ultrashort pulses in passive, uniform, photonic crystal fibers designed such that their nonlinear Kerr coefficient γ varies considerably with wavelength. Such fibers exhibit a zero-nonlinearity wavelength in addition to the zero-dispersion wavelength. We show that soliton evolution is affected considerably by the relative locations of the zero-nonlinearity and zero-dispersion wavelengths with respect to the input wavelength. Among the new features observed numerically are: the enhancement or suppression of the Raman-induced red-shift of fundamental solitons, amplification or suppression of a dispersive wave shed by the soliton, and the splitting of a fundamental soliton into two co-propagating solitons through a dispersive wave that forms a soliton in the normal-dispersion region because of a negative value of γ in this region.

PACS numbers: 42.81.Dp, 42.65.Ky, 42.65.-k

I. INTRODUCTION

It is well known that short optical pulse can propagate as solitons inside a nonlinear dispersive medium such as an optical fiber [1]. Fission of higher-order solitons into multiple fundamental (first-order, $N = 1$) solitons has been found useful for supercontinuum generation in optical fibers [2–4]. However, fundamental solitons themselves are resistant to fission or any kind of splitting [1, 5]. Generally, splitting of a fundamental soliton is only possible if the fiber is tapered [6–8] or is doped and pumped to provide amplification [9–12]. Both of these methods rely on increasing the soliton order to beyond $N = 1.5$ so that a second-order soliton is formed that splits into two fundamental solitons.

In this article we study numerically the evolution of ultrashort pulses in passive, uniform, photonic crystal fibers (PCFs) designed such that their nonlinear Kerr coefficient γ varies considerably with wavelength. This kind of strong frequency-dependence of the nonlinearity as well as negative nonlinearity [$\gamma(\omega) < 0$] have been demonstrated in fibers doped with silver nanoparticles [13, 14]. Indeed, in such fibers $\gamma(\omega)$ vanishes at a specific wavelength, called the zero-nonlinearity wavelength (ZNW), and changes its sign beyond that. A negative value of γ gives rise to nonlinear phenomena not commonly observed in conventional fibers. As an example, optical solitons can form even when a pulse experiences normal group-velocity dispersion (GVD). Here we study the evolution of fundamental solitons in PCFs exhibiting a ZNW in addition to the zero-dispersion wavelength (ZDW) and show that soliton dynamics are affected considerably by the relative locations of the ZNW and ZDW with respect to the input wavelength. In conventional PCFs with positive γ at all wavelengths, the ZDW separates a solitonic region from a non-solitonic one. As a result, any dispersive wave (DW) emitted by a soliton continues to disperse after crossing the ZDW boundary. The situation is different when the PCF has a ZNW close to the ZDW. In that case, the DW can form a soliton after crossing the ZDW boundary. The net effect is that energy of a single fundamental soliton appears to split into two parts propagating as solitons in different spectral regions. This process is different from soliton fission and bears resemblance to cellular mitosis in biology.

The paper is organized as follows. In Section 2 we introduce the propagation equation used for studying the soliton evolution and provide details of the numerical procedure used for this purpose. Section 3 shows how the frequency dependence of γ can enhance the spectral red-shift of solitons and suppress transfer of energy from it to a DW. Section 4 focuses on the dramatic changes in the soliton dynamics when the PCF has its ZDW and ZLW relatively close to the input wavelength. Splitting of a fundamental soliton into two solitons through a DW is studied in Section 5. The main conclusions are summarized in Section 6.

II. NUMERICAL MODEL

The propagation of short optical pulses is modeled well by the generalized nonlinear Schrödinger equation used commonly for simulating supercontinuum generation [1]. We convert this equation to the spectral domain and write it in the form

$$\frac{\partial \tilde{A}}{\partial z} - i[\beta(\omega) - \beta(\omega_0) - \beta_1(\omega - \omega_0)]\tilde{A} = i\gamma(\omega)(1 - f_R)\hat{\mathcal{F}}\left(|A|^2 A\right) + \gamma_0 f_R \times \hat{\mathcal{F}}\left(A \int_{-\infty}^{+\infty} h_R(t')|A(z, t - t')|^2 dt'\right), \quad (1)$$

where $\tilde{A}(z, \omega)$ is the Fourier transform of the pulse envelope and $\hat{\mathcal{F}}$ denotes the Fourier-transform operation. Also, h_R is the Raman response function of silica with $f_R = 0.18$ [1]. The frequency dependence of the nonlinear parameter is taken into account using

$$\gamma(\omega) = \gamma_0 + \gamma_1(\omega - \omega_0), \quad (2)$$

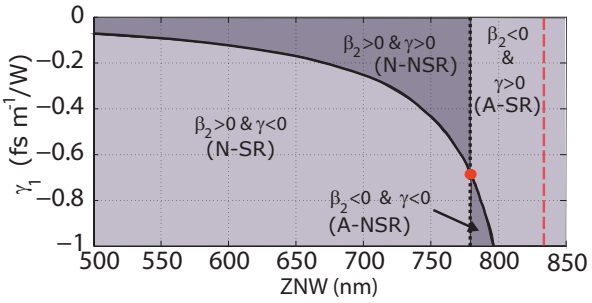

FIG. 1. γ_1 versus the ZNW for our PCFs (solid black line). The black vertical dashed line indicates the ZDW and the red vertical dashed line shows the pump wavelength. The red dot marks the point at which ZNW and ZDW coincide. The light gray areas indicate the solitonic region (SR) and the non-solitonic region (NSR) is shown in dark gray. The letters N and A refer to normal and anomalous GVD, respectively.

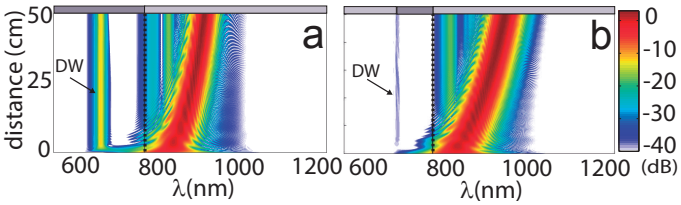

FIG. 2. Spectral evolutions of the 10 fs fundamental soliton inside a 50-cm-long PCF for $\gamma_1 = 0$ (a) and $\gamma_1 = -0.225$ fs $\cdot$ m^{-1}/W (b). The black dashed lines show the ZDW. The bars above the plots indicate the solitonic (lighter gray) and nonsolitonic (darker gray) regions.

where $\gamma_1 = d\gamma/d\omega$ is evaluated at the pump frequency ω_0. We assume γ_1 to be negative and vary it from 0 to -0.8 fs-m^{-1}/W. We assume that the Raman contribution is not affected by the mechanism used to modify the Kerr nonlinearity. The other parameters of the PCF are identical to those used in Ref. [15]. In particular $\gamma_0 = 0.11$ W^{-1}/m. The nonlinear parameter γ is inherently frequency-dependent in all optical fibers due to its dependence on the effective mode area $A_{\rm eff}$ ($\gamma = \omega_0 n_2/[cA_{\rm eff}(\omega)]$), and the dependence is characterized by the so-called shock time scale $\tau_{\rm shock} = 1/\omega_0$ such that $\gamma(\omega) = \gamma(\omega_0) + (\omega - \omega_0)/\omega_0$ [1]. This frequency-dependence leads to the well-known effects of soliton fission and self-steepening. The dependence of γ on the effective mode area can be used to tailor the the frequency-dependence of γ to a certain extent through careful engineering of the fiber refractive index profile. In practice this can mean novel photonic crystal fibers [3] or tapered fibers [16]. However, the effective area is not the only frequency-dependent quantity in the expression for γ. The nonlinear refractive index n_2, though weakly frequency-dependent for silica, can be strongly frequency-dependent for other materials. Hollow-core photonic crystal fibers offer a platform to utilize different gases for the fiber core material [17] and even a pressure gradient along the fiber [18], hence significantly changing the nonlinear properties of the fiber compared to silica. The most drastic changes, such as negative values of γ, can be induced by doping the fiber with metal nanoparticles, which is how the fibers studied here could be manufactured in practice [13, 14]. Such strong frequency-dependence is mathematically similar to the ordinary silica fiber nonlinearity that is responsible for self-steepening and optical shock effects, but it will demonstrated here that altering the magnitude of the frequency-dependence (the value of γ_1 in Eq. 2) will cause significant changes in the propagation dynamics of ultrashort pulses.

When $\gamma_1 < 0$, the Kerr nonlinearity vanishes at a specific frequency $\omega = \omega_0 - \gamma_0/\gamma_1$; ZNW is the wavelength corresponding to this frequency. The relation between γ_1 and ZNW is shown in Fig. 1, where the vertical black line shows the location of the PCF's ZDW and the dashed red line shows the pump wavelength of 835 nm. Solitons can exists at wavelengths for which $\gamma(\omega)$ and $\beta_2(\omega)$ have opposite signs. The wavelengths for which this condition is met are referred to as the solitonic region (SR); other wavelengths then belong to the non-solitonic region (NSR). Depending on the value of γ_1, the SR mights be disjoint and parts of the SR may have normal dispersion, as seen in Fig. 1.

To study pulse propagation in fibers with frequency-dependent nonlinearity, we solve Eq. (1) numerically using the fourth-order Runge–Kutta method. The 50 cm long PCF has its ZDW is at 780 nm. The input pulse at a wavelength of 835 nm with $A(0,t) = \sqrt{P_0}\,\mathrm{sech}(t/T_0)$ has a full width at half maximum of 10 fs. The peak power of the input pulse, $P_0 = 3.48$ kW, is chosen such that the soliton order is $N = T_0\sqrt{\gamma_0 P_0/|\beta_2|} = 1$ at the input end of the fiber. Contrary to a prevalent misconception, the GNLSE does not assume a slowly-varying pulse envelope and is accurate down to the single-cycle regime far from material resonance frequencies [3, 19].

III. INTRAPULSE RAMAN SCATTERING

It is well known that the spectrum of short solitons shifts to the red side because of intrapulse Raman scattering [1], a phenomenon referred to as the soliton self-frequency shift (SSFS). For positive values of the nonlinearity slope γ_1, this shift becomes smaller, resulting in the suppression of SSFS [20]. Since γ_1 is negative in our simulations, the nonlinear effects become enhanced as the soliton's spectrum is red-shifted. This leads to a variety of interesting effects, depending on the value of γ_1.

As an example, Fig. 2 compares the spectral evolutions of a 10 fs soliton inside two PCFs with $\gamma_1 = 0$ and -0.225 fs-m^{-1}/W. The $\gamma_1 = 0$ case shown in part (a) displays typical soliton dynamics. One sees the formation of a DW near 680 nm within the first few centimeters, followed by a continuous shift of the soliton spectrum toward the

red side, with some pump energy left at the input wavelength. This scenario is modified considerably in part (b) where $\gamma_1 < 0$. The soliton's red shift is enhanced considerably. But, most remarkably, the DW is almost completely suppressed. The most likely explanation for the DW suppression is that the soliton moves out of the phase-matching spectral region so quickly that little energy can be transferred to the DW. The SSFS enhancement and DW suppression certainly appear to be connected. In fact, the specific value $\gamma_1 = -0.225$ fs-m^{-1}/W was chosen because it leads to both the largest red shift and the least intense DW. Furthermore, for $\gamma_1 = -0.225$ fs-m^{-1}/W the DW frequencies are very close to the ZNW meaning that these frequencies experience smaller nonlinear effects which might hinder power transfer to them.

IV. AMPLIFICATION OF DISPERSIVE WAVES

The pulse evolution becomes drastically different when γ_1 has values between -0.325 and -0.375 fs-m^{-1}/W. Figure 3 shows the temporal and spectral evolutions for three different fibers having $\gamma_1 = -0.325$ (top row), -0.35 (middle row) and -0.375 fs-m^{-1}/W (bottom row). The spectrograms at the output of the fiber in each case are shown is the last column. For $\gamma_1 = -0.325$ fs-m^{-1}/W (top row), a DW is formed within the first few centimeters, once the phase-matching condition is fulfilled, and it is located in the N-SR region. This DW is trapped by the soliton and both decelerate together, as also evident in the spectrogram. The constant blue shift of the DW is the result of its deceleration in the normal-GVD regime so that its speed matches with that of the soliton. Notice that the DW also gains energy from the soliton as it propagates down the fiber.

The preceding scenario changes considerably for $\gamma_1 = -0.35$ fs-m^{-1}/W (middle row in Fig. 3). During the first half of the PCF length, we observe the red-shift of the soliton and the blue-shift of the DW, similar to the top row. However, in the second half of the PCF the red shift of the soliton turns into a blue shift. The DW is still trapped and it red shifts its spectrum, but the two move closer in time. Moreover, the intensity of the DW becomes considerably larger, and it becomes even more intense than the soliton after 30 cm of propagation. These features are a manifestation of several different effects acting together. First, it is known that self-steepening can amplify a DW [21]. Second, energy can be transferred from the soliton to the DW through temporal reflections [22], which are especially evident around 25 cm of propagation in the middle row of Fig. 3). Third, the more the soliton red shifts, the larger the value of γ it experiences. This means that the soliton must decrease its width, or peak power, or both to maintain $N = 1$, which can force the soliton to shed off some of its energy in the form of a DW. This only happens for strongly frequency-dependent nonlinearity for which the change in γ at the soliton's central frequency is too rapid for the soliton to adjust to adiabatically.

The last row of Fig. 3) shows what happens when γ_1 is made even more negative by choosing $\gamma_1 = -0.375$ fs-m^{-1}/W. Both the amplification of the DW and the blue shift of the soliton after 20 cm become stronger to the extent that their spectra appear to merge together at the PCF output. For this value of γ_1, a considerable part of soliton's energy is transferred to the DW such that its spectrum becomes narrower and is blue-shifted as the DW becomes more intense. Indeed, the DW now consists of two different frequency bands separated by the ZNW, as seen in spectrogram. This further indicates that energy transfer from the soliton to frequencies where the nonlinear parameter γ is close to zero is not efficient even when the phase matching condition is fulfilled. The vast majority of the DW energy is still on the blue side of the ZNW. The temporal evolution on the left shows that the soliton has returned to its original position and is considerably wider because of its energy loss. Although the DW has more energy, this energy is spread out over a much wider temporal window compared to the soliton. These features are also evident in the spectrogram where we also see a second DW emitted by the soliton on the red side.

V. FORMATION OF TWO SOLITONS

We have seen in Fig. 3) how a fundamental soliton emits a DW and subsequently amplifies for negative values of γ_1 near $\gamma_1 = -0.35$ fs-m^{-1}/W. The question we ask is whether this amplified DW can form a second soliton if γ_1 is made even more negative. The DW needs to be in the solitonic region of the spectrum where both γ and β_2 have opposite signs. The size of the solitonic spectral region can be increased by making the γ_1 even smaller (larger in magnitude). In this case, the input soliton can transfer a large portion of its energy to new frequencies in the solitonic region on the blue side of both the ZDW and the ZNW. Figure 4 compares the temporal and spectral evolutions of the 10 fs input pulse for $\gamma_1 = -0.6$ (top row), and -0.7 (bottom row) fs-m^{-1}/W. The spectrograms at the output of the fiber are shown in the right column. For both values of γ_1, the input spectrum lies on both sides of the ZNW and the ZDW, and the splitting of the initial pulse leads to two solitons and multiple dispersive waves. For $\gamma_1 = -0.6$ fs-m^{-1}/W (top row) one of the solitons is in the anomalous-GVD regime, and the other one is in the normal-GVD region. However, it is noteworthy, and even counterintuitive, that when the ZDW and ZNW coincide (bottom row of Fig. 4), both solitons at the fiber output are on the same side of the ZNW, where the GVD is anomalous.

The reason for the differences in the spectra of the two forming solitons in the two cases shown in Fig. 4 has to do with the temporal dynamics of the solitons. In the temporal trace for $\gamma_1 = -0.7$ fs-m^{-1}/W, the two solitons pass through one another during their first collision, whereas

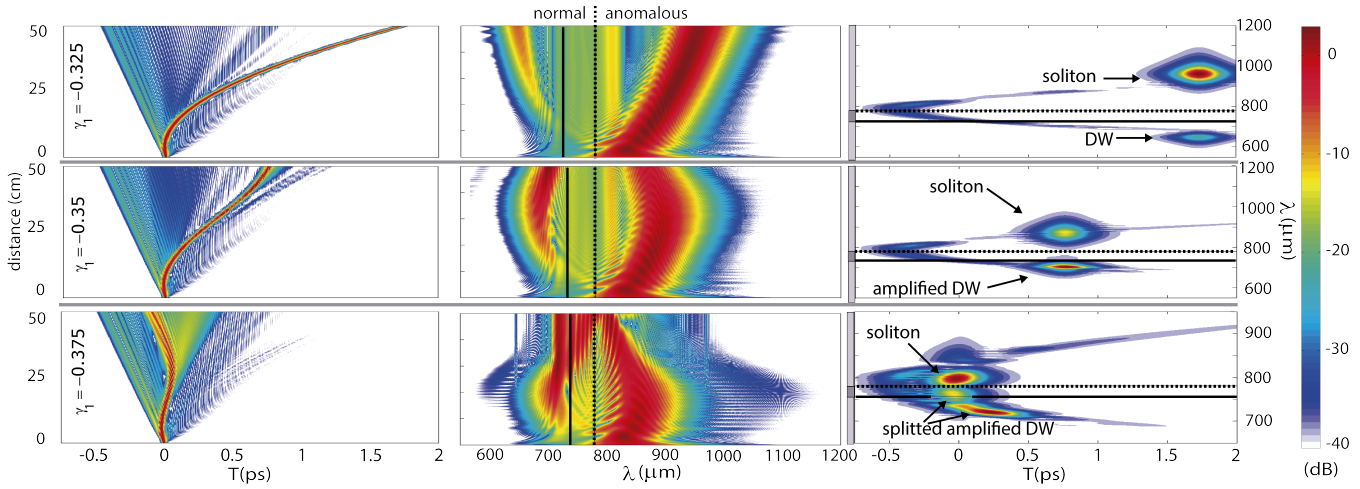

FIG. 3. Temporal (left) and spectral (middle) evolutions of a 10-fs soliton inside a 50-cm-long PCF for $\gamma_1 = -0.325$ (upper row), -0.35 (middle row) and -0.375 (lower row) fs-m^{-1}/W. The normalization is with respect to the input peak power that corresponds to 0 dB. Spectrograms at the PCF output are shown in right column for each case. Solid and dashed black lines mark the ZNW and the ZDW, respectively. Note the smaller wavelength range in the last spectrogram. The side bars in the spectrograms indicate the solitonic (lighter gray) and nonsolitonic (darker gray) regions.

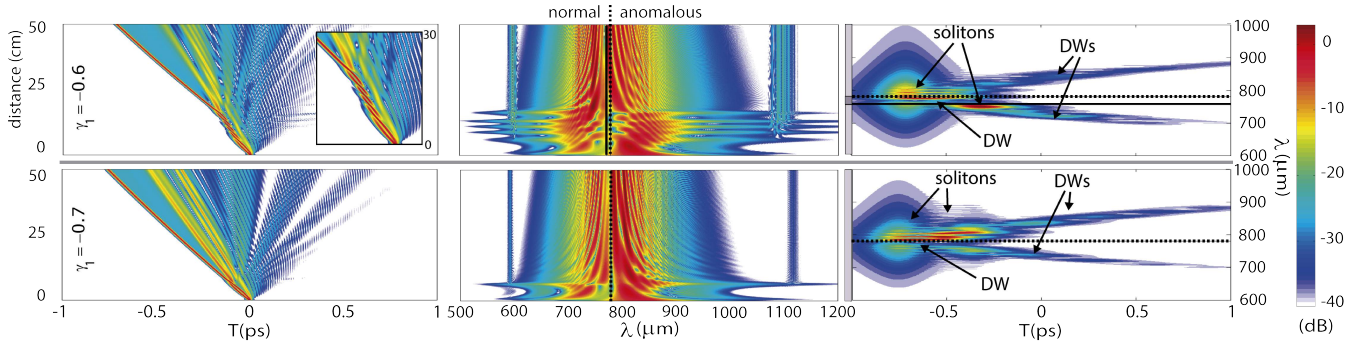

FIG. 4. Temporal (first column), and spectral (second column) evolutions of the fundamental soliton inside a 50-cm-long PCF for $\gamma_1 = -0.6$ (upper row), and -0.7 (lower row) fs-m^{-1}/W (the last chosen such that the ZNW coincides with the ZDW). The input peak power corresponds to 0 dB. The spectrograms at the PCF output are shown in third column for each case. Solid and dashed lines represent the ZNW and the ZDW, respectively. Note that the dispersive waves around 600 nm and 1100 nm have been delayed by 7 ps and hence are not visible in the spectrogram.

for $\gamma_1 =$ fs-m^{-1}/W the solitons interact and collide multiple times before one of the solitons gains most of the power and breaks free. The outcomes of such solitonic interactions can be very different depending on the relative phases of the solitons [23], and this phase sensitivity can explain some of the differences seen in the two cases in Fig. 4. In-phase collisions lead to narrow high-intensity pulses and the associated spectral broadening. A DW is emitted during each collision and more intense DWs lead to higher spectral recoil which can push the solitons in the opposite direction in the spectrum [24, 25]. An intense DW on the red side then means that the soliton gets pushed towards the blue.

Decreasing γ_1 below -0.7 fs/W/m brings the ZNW to the red side of the ZDW and brings it closer to the pump. The top row in Fig. 5, shows the temporal and spectral evolutions for a PCF with $\gamma_1 = -0.8$ fs/W/m. The non-solitonic region between the ZNW and the ZDW is now 7 nm wide. The bottom row shows the same case without including the the Raman contribution. This helps in isolating the role of the Raman effects.

Similar to Fig. 4, the soliton splits into two temporally separated pulses of different group velocities. The inset in Fig. 5 shows how the solitons separate from one another right at the input. The spectra of the individual pulses remain almost unchanged after the initial transient evolution, and changes in the spectrum with distance are a manifestation of the increasing temporal separation between the solitons and the corresponding DWs. When the Raman effect is off (lower row of Fig. 5) the DWs between the solitons disappear, but other than that and a slight change in the solitons' group velocities, the cases

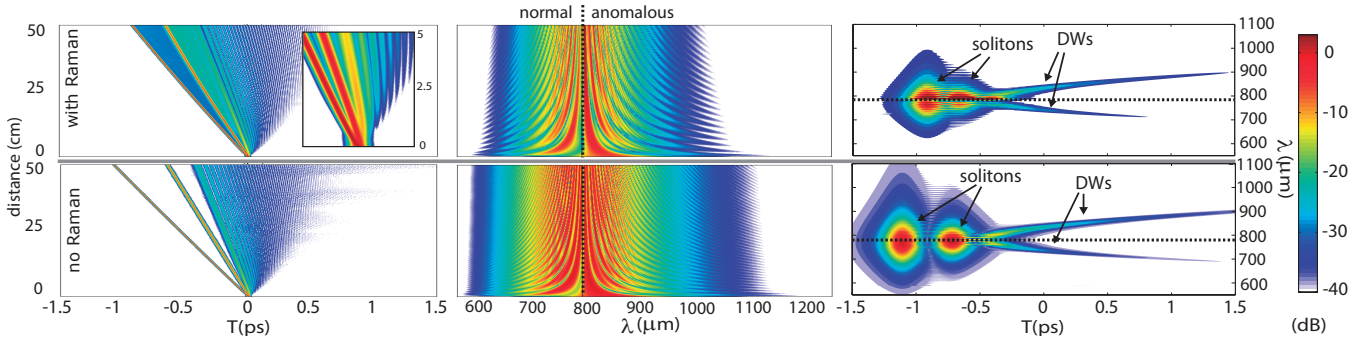

FIG. 5. Temporal (left) and spectral (middle) evolutions of a 10-fs soliton inside a 50-cm-long PCF for $\gamma_1 = -0.8$ fs-m^{-1}/W. The input peak power corresponds to 0 dB. The spectrogram at the PCF output is shown in the third column. The Raman contribution is turned off for the case shown in the bottom row. The ZNW and the ZDW are separated by ~ 7 nm in this case and the dashed line now represents this 7 nm window.

with and without Raman look quite similar. In a conventional fiber, SSFS bends the solitons' trajectories, which straighten if the Raman effect is turned off. Here, the trajectories are straight lines whether or not Raman is included, which indicates that the frequency-dependence of the nonlinearity has suppressed the SSFS almost completely.

VI. CONCLUSIONS

We have studied numerically the evolution of ultrashort optical pulses in passive, uniform, PCFs designed such that their nonlinear Kerr coefficient γ varies considerably with wavelength. In particular, we focused on the case in which γ decreases linearly with increasing frequency such that the Kerr nonlinearity changed its nature from self-focusing to self-defocusing beyond a certain frequency. Such fibers exhibit a zero-nonlinearity wavelength in addition to the zero-dispersion wavelength. We found that soliton evolution is affected considerably by the relative locations of the zero-nonlinearity and zero-dispersion wavelengths with respect to the input wavelength.

Our numerical results include both the Kerr and Raman nonlinearities together with self-steepening because of the femtosecond nature of the input pulse. We also include a realistic dispersion profile for the PCF. As a result, the spectrum of a fundamental soliton shifts to the red side through SSFS, as the soliton also sheds some energy in the form of a DW. One interesting feature we observe is the enhancement of the Raman-induced redshift of fundamental solitons. This is understood by noting that the Kerr nonlinearity is enhanced in our PCF at longer wavelengths. However, our numerical results show that the SSFS enhancement nearly suppresses the DW when the dispersion slope is negative but not too large in magnitude. With a further increase in its magnitude, the SSFS enhancement turns into SSFS suppression that is accompanied by an amplification of the DW shed by the soliton. Moreover, the DW is trapped by the soliton, and its spectrum moves closer to that of the soliton, resulting in spectral compression at the PCF output. These features are found to be quite sensitive to the exact numerical value of the nonlinearity slope γ_1; even a 10% change in its value can produce dramatic changes in both the time and spectral domains.

When the magnitude of dispersion slope is increased further (keeping it negative), a further change occurs in the soliton dynamics. The amplified DW now becomes so strong that it forms a fundamental soliton and creates its own DW, even though it lies in the normal-GVD region. The region behind it becomes clear by noting that the nonlinear γ has become negative in this spectral region, allowing for a soliton to form. This is interesting from a fundamental perspective because the energy of a fundamental soliton appears to split into two wider solitons. Of course, the splitting is not direct because it occurs through a DW that forms a soliton in the normal-dispersion region because of a negative value of γ_1 in this region. The important takeaway is that soliton dynamics becomes quite complex when the Kerr nonlinearity becomes strongly dispersive and leads to the presence of a ZNW in addition to the ZDW. Since the relative positions of these two wavelengths can be tailored through suitable design changes, such PCFs are suitable for a variety of practical applications.

FUNDING

Arteaga-Sierra: Funds National Council of Science and Technology (CONACyT) post-doctoral grant (277594); Antikainen: Väisälä Fund graduate study grant of the Finnish Academy of Science and Letters. Agrawal: National Science Foundation grant ECCS-1505636.

[1] G. P. Agrawal, *Nonlinear Fiber Optics*, 5th ed. (Academic, 2013).

[2] A. V. Husakou and J. Herrmann, "Supercontinuum Generation of Higher-Order Solitons by Fission in Photonic Crystal Fibers," Phys. Rev. Lett. **87**, 203901 (2001.)

[3] J. M. Dudley, G. Genty, and S. Coen, "Supercontinuum generation in photonic cristal fibers," Rev. Mod. Phys. **78**, 1135–1184 (2006).

[4] V. Skryabin and A. V. Gorbach, "Colloquium: Looking at a soliton through the prism of optical supercontinuum," Rev. Mod. Phys. **82**, 1287–1299 (2010).

[5] N. Akhmediev and A. Ankiewicz, *Solitons: Non-linear pulses and beams*, (Chapman and Hall, 1997).

[6] T. A. Birks, W. J. Wadsworth, and P. St. J. Russell, "Supercontinuum generation in tapered fibers," Opt. Lett. 25, 1415–1417 (2000).

[7] W. J. Wadsworth, A. Ortigosa-Blanch, J. C. Knight, T. A. Birks, T.-P. Martin Man, and P. St. J. Russell, Supercontinuum generation in photonic crystal fibers and optical fiber tapers: a novel light source, J. Opt. Soc. Am. B 19, 2148–2155 (2002).

[8] F. R. Arteaga-Sierra, C. Milián, I. Torres-Gómez, M. Torres-Cisneros, A. Ferrando, and A. Dávila, "Multipeak-spectra generation with Cherenkov radiation in a non-uniform single mode fiber," Opt. Express 22, 2451–2458 (2014)

[9] P. H. Pioger, V. Couderc, P. Leproux, and P. A. Champert, "High spectral power density supercontinuum generation in a nonlinear fiber amplifier" Opt. Express 15, 11358 (2007)

[10] R. Song, J. Hou, S. Chen, W. Yang, and Q. Lu, "High power supercontinuum generation in a nonlinear ytterbium-doped fiber amplifier," Opt. Lett. 37, 1529 (2012)

[11] M. Tao, T. Yu, Z. Wang, H. Chen, Y. Shen, G. Feng, and X. Ye, "Super-flat supercontinuum generation from a Tm-doped fiber amplifier," Sci. Rep. 6, 23759 (2016)

[12] F. R. Arteaga-Sierra, A. Antikainen, and Govind P. Agrawal, "Dynamics of soliton cascades in fiber amplifiers," Opt. Lett. 41, 5198–5201 (2016)

[13] R. Driben, A. Husakou, and J. Herrmann, "Low-threshold supercontinuum generation in glasses doped with silver nanoparticles," Opt. Express **17**, 17989–17995 (2009).

[14] S. Bose, R. Chattopadhyay, S. Roy, and S. K. Bhadra, "Study of nonlinear dynamics in silver-nanoparticle-doped photonic crystal fiber," J. Opt. Soc. Am. B **33**, 1014–1021 (2016).

[15] J. K. Ranka, R. S. Windeler, and A. J. Stentz, "Visible continuum generation in air-silica microstructure optical fibers with anomalous dispersion at 800 nm," Opt. Lett. **25**, 25–27. (2000).

[16] S. P. Stark, J. C. Travers, and P. St. J. Russell, "Extreme supercontinuum generation to the deep UV," Opt. Lett. **37**(5), 770–772 (2012)

[17] M. F. Saleh, W. Chang, P. Hölzer, A. Nazarkin, J. C. Travers, N. Y. Joly, P. St. J. Russell, and F. Biancalana, "Theory of Photoionization-Induced Blueshift of Ultrashort Solitons in Gas-Filled Hollow-Core Photonic Crystal Fibers," Phys. Rev. Lett. **107**, 203902 (2011).

[18] J. Lægsgaard and P. J. Roberts, "Theory of adiabatic pressure-gradient soliton compression in hollow-core photonic bandgap fibers," Opt. Lett. **34**(23), 3710–3712 (2009)

[19] T. Brabec and F. Krausz, "Nonlinear Optical Pulse Propagation in the Single-Cycle Regime," Phys. Rev. Lett. **78**(17), 3282–3285 (1997)

[20] O. Vanvincq, A. Kudlinski, A. Bétourné, Y. Quiquempois, and G. Bouwmans, "Extreme deceleration of the soliton self-frequency shift by the third-order dispersion in solid-core photonic bandgap fibers," J. Opt. Soc. Am. B **27**, 2328–2335 (2010)

[21] H. Liu, Y. Dai, C. Xu, J. Wu, K. Xu, Y. Li, X. Hong, and J. Lin, "Dynamics of Cherenkov radiation trapped by a soliton in photonic-crystal fibers," Opt. Lett. 35, 4042–4044 (2010)

[22] A. Antikainen, F. R. Arteaga-Sierra, G. P. Agrawal, "Temporal reflection as a spectral-broadening mechanism in dual-pumped dispersion-decreasing fibers and its connection to dispersive waves," Phys. Rev. A **95**, 033813 (2017)

[23] A. Antikainen, M. Erkintalo, J. M. Dudley, and G. Genty, "On the phase-dependent manifestation of optical rogue waves," Nonlinearity **25**(7), R73 (2012)

[24] G. R. Boyer and X. F. Carlotti, "Nonlinear propagation in a single-mode optical fiber in case of small group velocity dispersion," Optics Communications **60**(1,2) 18–22 (1986)

[25] P. K. A. Wai, C. R. Menyuk, H. H. Chen, and Y. C. Lee "Soliton at the zero-group-dispersion wavelength of a single-model fiber," Optics Letters **12**(8) 628–630 (1987)